

Efficient Cover Construction for Ball Mapper via Accelerated Range Queries

Efficient Range Queries for Large-Scale Data

Jay-Anne Bulauan

bulauan_jayanne@yahoo.com
Independent Researcher

John Rick Manzanares

jdolormanzanares@impan.pl
Dioscuri Centre in Topological Data Analysis, Institute of
Mathematics of the Polish Academy of Sciences /
International Environmental Doctoral School of the
University of Silesia in Katowice

Abstract

Ball Mapper is a widely used tool in topological data analysis for summarizing the structure of high-dimensional data through metric-based coverings and graph representations. A central computational bottleneck in Ball Mapper is the construction of the underlying cover, which requires repeated range queries to identify data points within a fixed distance of selected landmarks. As data sets grow in size and dimensionality, naive implementations of this step become increasingly inefficient.

In this work, we study practical strategies for accelerating cover construction in Ball Mapper by improving the efficiency of range queries. We integrate two complementary approaches into the Ball Mapper pipeline: hierarchical geometric pruning using ball tree data structures, and hardware-aware distance computation using Facebook AI Similarity Search. We describe the underlying algorithms, discuss their trade-offs with respect to metric flexibility and dimensionality, and provide implementation details relevant to large-scale data analysis.

Empirical benchmarks demonstrate that both approaches yield substantial speedups over the baseline implementation, with performance gains depending on data set size, dimensionality, and choice of distance function. These results improve the practical scalability of Ball Mapper without modifying its theoretical formulation and provide guidance for the efficient implementation of metric-based exploratory tools in modern data analysis workflows.

Keywords: Metric Tree, Simplicial Complex, Nerve

1. Introduction

The rapid growth of high-dimensional and large-scale data has created significant challenges for modern data analysis pipelines. As datasets increase in both size and dimensionality, many traditional geometric and statistical tools become inefficient or unreliable. This phenomenon is commonly referred to as the *curse of dimensionality* [1]. In such settings, distances between points become less informative, nearest-neighbour searches grow increasingly expensive, and classical algorithms often fail to scale to contemporary data volumes. These challenges moti-

vate the development of methods that extract meaningful structure from complex data while remaining computationally tractable.

Topological Data Analysis (TDA) offers one such framework by shifting the focus from precise coordinate representations to the qualitative shape of data. Among its established tools, the Ball Mapper algorithm [2] provides a coarse topological summary by constructing a graph from a metric cover of the dataset and the intersections between covering sets. The resulting representation highlights clusters and connectivity patterns, making Ball Mapper a practi-

cal and interpretable tool for exploratory analysis in high-dimensional settings.

Despite its conceptual robustness, the practical performance of Ball Mapper is strongly influenced by the construction of the underlying cover. In high-dimensional and large-scale settings, where the method is most appealing, this step becomes a significant computational bottleneck. In particular, the current implementation *pyBallMapper* (<https://github.com/dioscuri-tda/pyBallMapper>) relies on relatively straightforward distance-search routines that do not fully exploit advanced data structures or optimized libraries. As a result, scalability limitations increasingly restrict the algorithm’s applicability to real-world big-data scenarios.

In this study, we address this limitation by improving the cover construction phase of the Ball Mapper pipeline through the inegration of more efficient nearest-neighbour search mechanisms. We evaluate their performance, discuss key implementation details, and examine the implications for scaling Ball Mapper to larger and more complex datasets. Rather than proposing a new variant of the algorithm, our goal is to strengthen the practical performance of its existing implementation and to provide guidance for the development of efficient metric-based tools for large-scale data analysis.

2. Ball Mapper

This section introduces the Ball Mapper framework. We first present the theoretical background underpinning the method, then describe the construction of the ε -net and associated graph, and finally discuss the coloring schemes used to encode and analyze auxiliary data.

2.1. Theory

To describe the Ball Mapper algorithm rigorously, we first outline the mathematical setting in which it operates. First, we model the dataset as a metric space. A metric space (X, d) is a set X together with a *distance function* $d : X \times X \rightarrow \mathbb{R}$ satisfying, for all $x, y, z \in X$,

1. $d(x, y) \geq 0$ (non-negativity),
2. $d(x, y) = 0$ if and only if $x = y$ (identity of indiscernibles),
3. $d(x, y) = d(y, x)$ (symmetry), and

4. $d(x, z) \leq d(x, y) + d(y, z)$ (triangle inequality).

Given a metric structure on the dataset, the next step is to select a finite set of representative points that captures the geometry of the space at a prescribes scale. This is achieved through the notion of an ε -net.

Definition 2.1. Let (X, d) be a metric space. For a real number $\varepsilon > 0$, an ε -net of X is a subset $N \subset X$ satisfying:

1. For every point $x \in X$, there exists $n \in N$ with $d(x, n) < \varepsilon$.
2. For any pair of distinct points $n_1, n_2 \in N$, we have $d(n_1, n_2) \geq \varepsilon$.

Elements of N are called *landmarks*.

An ε -net naturally induces a collection of neighborhoods by associating to each landmark a ball of radius ε . Specifically, an ε -net $\{c_1, c_2, \dots, c_k\}$ yields a collection of *open balls* of radius ε

$$B(c_i, \varepsilon) = \{y \in X \mid d(x, y) < \varepsilon\}.$$

centered at the landmarks c_i . The union of these balls is said to *cover* the metric space X .

The parameter ε controls the scale at which the metric structure of the dataset is examined. Smaller values of ε produce covers with more balls of smaller radius, yielding a finer representation of local geometric features. Larger values result in coarser covers in which local variations are aggregated. In practice, ε is chosen to balance resolution against robustness to sampling noise.

Given a cover of the dataset, a standard way to encode the pattern of overlaps among the covering sets is through an abstract simplicial complex. This construction records not only pairwise intersections but also higher-order overlaps in a combinatorial form.

An (*abstract*) *simplicial complex* is a pair (V, S) where V is a set of *vertices*, and S is a collection of non-empty finite subsets of V satisfying the following:

1. For every $v \in V$, $\{v\} \in S$.
2. If $\sigma \in S$ and $\tau \subset \sigma$, then $\tau \in S$.

Elements σ of S are called *k-simplices* where the *dimension* $k = |\sigma| - 1$.

Definition 2.2. The *nerve* of the cover induced by an ε -net is the abstract simplicial complex defined as follows. The vertex set consists of the landmarks

$\{c_1, \dots, c_k\}$. A finite subset $\{c_{\{i_0\}}, \dots, c_{\{i_m\}}\}$ of landmarks spans an m -simplex if the corresponding open balls of radius ε have a non-empty common intersection, that is,

$$\bigcap_{j=0}^m B(c_{i_j}, \varepsilon) \cap X \neq \emptyset.$$

A k -skeleton of a simplicial complex S is a simplicial complex containing all simplices of S whose dimension at most k . The *Ball Mapper graph* is the 1-skeleton of the nerve of an ε -net. The 0-simplices (or *vertices*) are precisely the landmarks, while the 1-simplices (or *edges*) between two vertices are formed when the associated landmarks have a nonempty intersection.

While higher-order simplices encode multiway intersections among balls, restricting attention to the 1-skeleton yields a graph representation that is computationally efficient and easy to interpret. This representation preserves the dominant pairwise connectivity structure and is well-suited to exploratory analysis and visualization.

In algebraic topology, the Nerve Lemma [3] states that, under suitable conditions, the nerve of a cover accurately reflects the global shape of the underlying space. These conditions are generally not satisfied as the Ball Mapper is constructed from a finite data sample rather than the full metric space. As a consequence, the resulting graph should be interpreted as a descriptive summary of the data rather than a topologically exact representation of the underlying space.

2.2. ε -Net Construction

In practice, Ball Mapper constructs a cover of a finite dataset X by computing an ε -net using a greedy algorithm. The procedure is as follows:

1. Initialize an empty set N to hold the landmarks.
2. While there exist uncovered points in the dataset:
 - Select an uncovered point x from the dataset.
 - Add x to N .
 - Mark all points within distance ε of x as covered.

A point is said to be *covered* if it lies within at least one ball centered at a landmark in N ; otherwise, it is *uncovered*.

This greedy construction depends on the order in which points are processed, and consequently the resulting set of landmarks is not unique. An alternative approach is *farthest point sampling* [4], which produces a deterministic ε -net. The procedure is as follows:

1. Select an initial landmark $x_0 \in X$.
2. Initialize a set L to hold the current landmark set.
3. Find a point

$$x^* = \arg \max_{x \in X} \min_{l \in L} d(x, l)$$

farthest from the current landmark set.

4. Add x^* to L if $\min_{l \in L} d(x^*, l) > \varepsilon$.
5. Repeat until no such point exists.

This procedure yields a unique landmark set for a given dataset and distance metric. However, it is typically more computationally expensive than the greedy algorithm and is therefore less commonly used in large-scale applications.

2.3. Coloring

In applications, the Ball Mapper is typically used as a scaffold for visualizing auxiliary information associated with the data, such as response variables, labels, or summary statistics. By aggregating such quantities over balls, one can examine how they vary across regions of the data space while respecting its metric structure.

Let M be a Ball Mapper graph with landmark set L . A *coloring* of M is a function $c : L \rightarrow \mathbb{R}$ where $c(l)$ encodes aggregated information associated with the open ball centered at $l \in L$.

Let $f : X \rightarrow \mathbb{R}$ be a real-valued function defined on the dataset X . For example, f can be some response variable or feature. Given a landmark l_i of M , let $X_i = X \cap B(l_i, \varepsilon)$. A common choice of coloring is given by averaging:

$$c(l_i) = \frac{1}{|X_i|} \sum_{x \in X_i} f(x)$$

This assigns to each vertex a summary statistic of the data points contained in its corresponding ball.

To understand how coloring behaves across the graph, we impose a mild regularity assumption on f . Note that \mathbb{R} can be viewed as a metric space with the Euclidean distance function $|\cdot|$.

Definition 2.3. The function f is said to be k -Lipschitz continuous if, for some constant k ,

$$|f(x) - f(y)| \leq kd(x, y)$$

for all $x, y \in X$.

For a Lipschitz continuous function, the difference in the images of any two points is at most proportional to the distance between the points.

Proposition 2.4. Let f be a k -Lipschitz continuous real-valued function defined on a finite metric space X and c is a coloring such that

$$\min_{x \in X_i} f(x) \leq c(l_i) \leq \max_{x \in X_i} f(x).$$

Then, for any landmark l_i of a Ball Mapper graph M , we have

$$\max_{x \in X_i} |f(x) - c(l_i)| \leq k\varepsilon.$$

Proof. Suppose f is k -Lipschitz continuous. Then, for some constant k ,

$$|f(x) - f(y)| \leq kd(x, y)$$

for all $x, y \in X$. The same equation holds for X_i . Thus, for $x_i \in X_i$, we have

$$|f(x) - f(x_i)| \leq kd(x, x_i) < k\varepsilon$$

for all $x \in X_i$. Consequently,

$$|f(x) - c(l_i)| \leq \max_{y \in X_i} |f(x) - f(y)| \leq k\varepsilon.$$

This proves the proposition. \square

Note that taking the mean for the coloring satisfies the assumption of [Proposition 2.4](#). Taking the median, trimmed mean, maximum and minimum also satisfies this. However, taking the variance or range do not satisfy this.

[Proposition 2.4](#) assures that, under suitable conditions, the color of a vertex cannot vary by more than $k\varepsilon$ for the chosen ε in the Ball Mapper construction.

Proposition 2.5. Let f be a k -Lipschitz continuous real-valued function defined on a finite metric space X and c is a coloring such that

$$\min_{x \in X_i} f(x) \leq c(l_i) \leq \max_{x \in X_i} f(x).$$

If (l_i, l_j) is an edge of a Ball Mapper graph, then

$$|c(v_i) - c(v_j)| \leq 2k\varepsilon.$$

Proof. An edge is spanned in a Ball Mapper graph when the open balls have a nonempty intersection. Let x be an element of this intersection. This also means that $x \in X_i$ and $x \in X_j$. The conclusion directly follows from using the triangle inequality

$$|c(v_i) - c(v_j)| \leq |c(v_i) - f(x)| + |f(x) - c(v_j)|$$

and applying [Proposition 2.4](#). \square

[Proposition 2.5](#) guarantees that, under the same conditions as [Proposition 2.4](#), the color difference between adjacent vertices is bounded by the maximum variation inside their overlapping region. Both propositions justify that Ball Mapper coloring is smooth over the graph: nearby vertices have similar colors.

When the function fails to be Lipschitz continuous, sharp color transitions naturally arise, and the Ball Mapper graph instead acts as a segmentation tool, identifying regions of qualitatively different behavior. This may happen, for example, when f represents class labels in classification problems. In such cases, robust or categorical summaries such as the mode or majority vote are often more appropriate than averaging-based colorings.

In both perspectives, the choice of coloring determines the role played by the Ball Mapper. Smooth colorings emphasize geometric continuity, while non-smooth colorings expose boundaries and regimes. Neither viewpoint is preferable a priori; each answers a different question about the data.

Lastly, the coloring depends on the choice of landmarks. The greedy ε -net construction is order-dependent and may yield non-unique landmark sets, resulting in non-consistent colorings, whereas landmark sets obtained via farthest point sampling are uniquely determined by the data and the parameter ε .

3. Efficient ε -Net Construction

Constructing an ε -net requires repeatedly identifying all points within distance ε of a selected landmark. This operation is known as a *range query*. When performed naively, range queries require computing distances from the query point to all points in the dataset, which becomes the dominant computational cost for large or high-dimensional datasets.

To mitigate this cost, a variety of data structures and computational techniques have been developed to accelerate range queries. In this section, we focus on two such approaches: hierarchical spatial data structures, exemplified by ball trees, and low-level algebraic optimizations, exemplified by Facebook AI Similarity Search (FAISS).

3.1. Tree-Based Acceleration

Data structures are used to store datasets in ways that make certain operations more efficient. Ball trees are hierarchical data structures designed to accelerate range queries in general metric spaces by recursively partitioning the dataset into nested metric balls.

A *tree* is a connected acyclic graph. A *rooted tree* is a tree with a distinguished node called the *root*, where edges are directed away from the root. A *binary tree* is a rooted tree in which each node has at most two children. Nodes with no children are called *leaves*.

A *ball tree* [5] is a rooted binary tree data structure where each node in the tree represents a ball that contains a subset of the data points. A Python implementation of the ball tree data structure is readily available through scikit-learn [6].

The following steps follow the scikit-learn’s implementation. Suppose we have a dataset (X, d) of dimension n . In a ball tree data structure, X is the root. We then compute the *center* $c := (c_1, \dots, c_n)$ where

$$c_i = \frac{\max(x_i) + \min(x_i)}{2}$$

and compute the radius defined by

$$r = \max_{x \in X} d(c, x).$$

Now, we find the point

$$p_A = \arg \max_{x \in X} d(c, x)$$

farthest from the center point c , and the point

$$p_B = \arg \max_{x \in X} d(p_A, x)$$

farthest from the p_A . Then, for each $x \in X$, collect all points closer to p_A than p_B into a collection X_A , and the rest into a collection X_B . Those subsets form the children nodes. Recursively, we repeat the same procedure for each child node until a stopping crite-

rion is met. In scikit-learn, the stopping criterion is when a node contains less than or equal to a specified number of points (default is 40).

The choice of leaf size introduces a trade-off between tree depth and query cost. Smaller leaf sizes result in deeper trees with tighter bounding balls, enabling more aggressive pruning during range queries, but incur greater traversal overhead. Conversely, larger leaf sizes produce shallower trees with looser bounds, reducing traversal cost but requiring more point-wise distance computations at the leaves. In practice, the optimal leaf size depends on the dataset size, dimensionality, and the cost of evaluating the chosen distance function.

The range query proceeds as follows. Given a query point q and a radius r , we start at the root node with center c and radius R . If the condition

$$d(q, c) - R > r$$

is satisfied, then $B(q, r) = \emptyset$. Otherwise, then there may be points in $B(q, r)$. This pruning condition follows directly from the triangle inequality and allows entire subtrees to be discarded without examining individual points. We then recursively visit each child node and perform the same check. If we reach the leaves, we check the distance of each point in the leaf to determine $B(q, r)$.

Ball trees support a wide range of metric including Euclidean, Manhattan, Jaccard, and general user-defined distance functions. This flexibility makes ball trees particularly suitable for metric-based algorithms such as Ball Mapper.

3.2. Algebraic Acceleration

For many commonly used metrics, distance computations admit algebraic decompositions that can be exploited for efficiency. We illustrate this for the Euclidean distance. Consider a fixed query point q and the squared Euclidean distance

$$d(q, x) = \left(\sum_j (q_j - x_j)^2 \right)^{\frac{1}{2}}.$$

The squared Euclidean distance can be expressed as

$$d^2(q, x) = d^2(q, 0) + d^2(x, 0) - 2 \sum_j q_j x_j.$$

The term $d^2(q, 0)$ is constant and computed only once per query. The term $d^2(x, 0)$ can be precomputed and stored. Consequently, the dominant cost in evaluating lies in the remaining term. This operation requires operations between q and each data point.

Facebook AI Similarity Search (FAISS) [7] accelerates this computation by exploiting two mechanisms: single instruction, multiple data (SIMD) processing [8] and basic linear algebra subprograms (BLAS) [9]. SIMD instructions allow the same arithmetic operation to be applied simultaneously to multiple components of a vector, enabling parallel evaluation of inner products at the hardware level. BLAS is a standardized interface whose implementations are extremely optimized engines for linear algebra. By expressing collections of inner products as matrix-vector or matrix-matrix operations, FAISS leverages highly-optimized BLAS routines that are tuned for modern CPU and GPU architectures.

As a result, FAISS reduces the constant factors associated with distance evaluation without altering the underlying algorithmic complexity. In contrast to tree-based data structures such as ball trees, which reduce the number of distance computations via geometric pruning, FAISS accelerates the cost per distance computation through low-level numerical optimization. Furthermore, parallelism of operations are allowed in FAISS which may further speedup computation with advanced hardware.

Unlike ball trees, however, FAISS is primarily designed for Euclidean distance and cosine similarity. While FAISS supports additional distance measures, these are typically handled through approximate or transformed representations rather than exact metric evaluations.

4. Benchmarking

We evaluate the computational performance of Ball Tree, FAISS, and pyBallMapper (pyBM). The benchmarking focuses on running time, relative speedup with respect to pyBallMapper, and memory usage. Additionally, we examine the empirical scaling behavior of each method to characterize how computational cost grows in practice.

All experiments were run on a machine with a 13th-generation Intel Core i5-13420H processor (2.10 GHz)

featuring 8 cores and 12 threads, and 16 GB of RAM. Computations were carried out on the CPU using integrated Intel UHD Graphics; no GPU acceleration was used. All methods were implemented in Python 3.12 with scikit-learn 1.7, FAISS 1.13, and pyBallMapper 0.3 libraries.

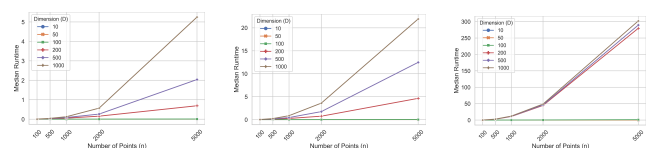
Datasets were generated to investigate the effects of dataset size and dimension. Across all experiments, the dataset size was set to $n \in \{100, 500, 1000, 2000, 5000\}$, and the dimension to $D \in \{10, 50, 100, 200, 500, 1000\}$, with 65 repeated trials conducted for each (n, D) combination.

In all experiments, the Euclidean distance is used for the ε -net construction. The leaf size of the Ball Tree data structure is set to 40, and FAISS is configured to allow up to 12 CPU threads. The main Python code is available through GitHub (<https://github.com/jhnrckmznrs/ballMapper>).

4.1. Runtime and Speedup Analysis

We investigate the runtime behavior and relative speedup of Ball Tree, FAISS, and pyBallMapper by examining how performance scales with problem size. We conduct a two-stage benchmarking procedure, first varying the number of data points n at fixed dimensionality, and then varying the dimensionality D at fixed dataset size.

Figure 1 reports the median runtime of the algorithms across the experimental conditions described above. The runtime of all methods increases with the number of data points n , though with markedly different scaling behavior. FAISS consistently exhibits the best runtime performance, maintaining low runtimes even as n becomes large. Ball Tree scales reasonably with n at fixed dimensionality, but shows higher runtimes than FAISS across all dataset sizes. In contrast, pyBallMapper displays a much steeper increase in runtime as n grows, becoming substantially more expensive for large datasets.



(a) FAISS (b) Ball Tree (c) pyBM
Figure 1: Median runtime of FAISS, Ball Tree, and pyBM across varying dataset sizes n .

Figure 2 illustrates the effect of increasing dimensionality on runtime. FAISS remains comparatively efficient even at high D , demonstrating strong robustness to increasing dimensionality. Ball Tree performs well at low dimensions but degrades rapidly as D increases, reflecting the impact of the curse of dimensionality on tree-based nearest-neighbor methods. pyBallMapper shows the most pronounced sensitivity to dimensionality, with runtimes increasing sharply and becoming especially costly for $D \geq 200$.

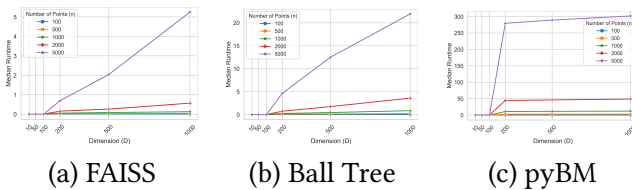


Figure 2: Median runtime of FAISS, Ball Tree, and pyBM across varying dimensions D .

While runtime provides insight into raw performance, it does not directly convey the relative computational advantage of alternative methods over a baseline. To better quantify how much faster FAISS and Ball Tree are compared to pyBallMapper under identical experimental conditions, we therefore report *speedup* of the proposed algorithm relative to pyBM, defined as the ratio between the runtime of proposed algorithm over the runtime of pyBM. This relative measure highlights how performance gaps evolve as problem size and dimensionality increase, and complements the absolute runtime analysis presented above.

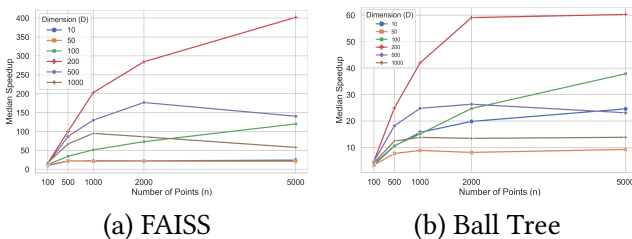


Figure 3: Median speedup of the proposed algorithms relative to pyBM across varying dataset sizes n .

Figure 3 shows the median speedup of FAISS and Ball Tree relative to pyBallMapper as the number of data points n increases. For both methods, speedup grows with n , indicating that the computational cost of pyBallMapper scales more rapidly with dataset size than that of the proposed approaches. FAISS exhibits the largest gains, achieving speedups exceeding two

orders of magnitude for large datasets, while Ball Tree shows consistent but more modest improvements across the range of n .

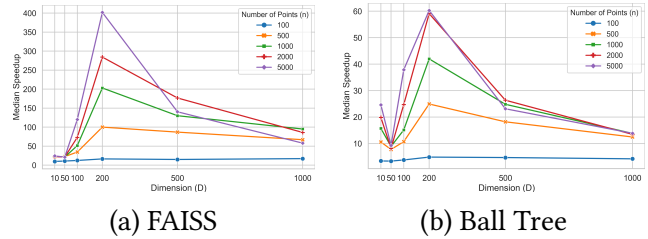


Figure 4: Median speedup of the proposed algorithms relative to pyBM across varying dimensions D .

As illustrated in Figure 4, speedup also increases with dimensionality D . This trend reflects the sharp degradation of pyBallMapper performance in high-dimensional settings. FAISS again achieves the most substantial improvements, reaching speedups of over two orders of magnitude at moderate to high dimensions (approximately 200). Ball Tree benefits from increased dimensionality as well, but to a lesser extent, consistent with its sensitivity to the curse of dimensionality.

Overall, these results indicate that FAISS is the most robust choice for large, high-dimensional datasets, particularly when sufficient parallel resources are available, as its performance depends on the number of threads used. This robustness is reflected in both low absolute runtimes and large speedups relative to pyBallMapper. Ball Tree is well suited for low-dimensional settings, although its runtime and relative performance are sensitive to the choice of leaf size, which can significantly affect query efficiency. In contrast, the steep runtime growth of pyBallMapper limits its practicality beyond small or low-dimensional regimes.

4.2. Memory Usage

We examine the memory requirements of the algorithms using *peak memory usage*. This refers to the maximum resident memory observed during execution and reported in megabytes (MB). This measure captures the largest memory footprint observed while the algorithm is running, including memory used for data structures, indexing, and intermediate allocations, but excluding memory that is freed before the peak is reached.

Figure 5 shows the median peak memory usage of the three methods as a function of dataset size n . For all algorithms, peak memory increases with n , reflecting the cost of storing data-dependent structures that scale with the number of points. FAISS exhibits the highest peak memory usage, particularly for large datasets, consistent with its reliance on dense vector representations and indexing structures optimized for fast search. Ball Tree remains relatively memory-efficient across all dataset sizes, with a more gradual increase in memory usage. pyBallMapper shows lower absolute memory consumption but still exhibits noticeable growth as n increases.

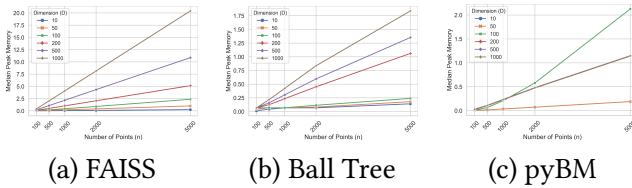


Figure 5: Median peak memory usage of the algorithms across varying dataset sizes n .

As shown in Figure 6, peak memory usage also increases with dimensionality D , though the sensitivity varies across methods. FAISS again shows the largest memory footprint at high dimensions, reflecting the cost of storing and processing high-dimensional dense vectors. Ball Tree displays comparatively modest growth in memory usage as D increases. In contrast, pyBallMapper, while maintaining lower overall memory usage, shows increased sensitivity to dimensionality, particularly at intermediate dataset sizes.

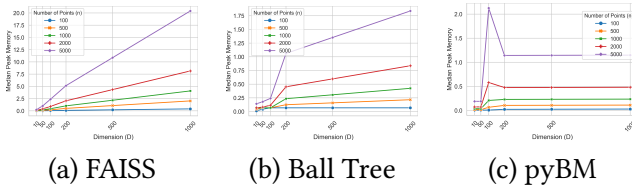


Figure 6: Median peak memory usage of the algorithms across varying dimensions D .

Overall, these results highlight a clear trade-off between computational speed and memory usage: FAISS achieves superior runtime performance at the cost of a larger memory footprint, while Ball Tree and pyBallMapper are more memory-efficient but incur higher runtimes in high-dimensional and large-scale settings. The increased memory footprint of FAISS reflects design choices that favor dense data represen-

tations and auxiliary indexing structures to maximize computational efficiency.

4.3. Complexity Analysis

To evaluate the computational complexity of each algorithm, we perform a log-log regression of the runtime $T(D)$ as a function of the dimension D . In this analysis, we assume that runtime follows a *power law* relationship of the form

$$T(D) = kD^p$$

for some constant k . Taking the logarithm of both sides yields

$$\log T(D) = \log k + p \log D,$$

which expresses $\log T(D)$ as a linear function of $\log D$. We estimate this linear relationship using least-squares regression, and the coefficient p is interpreted as the *empirical scaling exponent*. A value of $p = 1$ corresponds to linear growth in runtime with respect to the dimension, while $p = 2$, indicates quadratic scaling.

The quality of the fit is assessed using the *coefficient of determination* R^2 defined as

$$R^2 = 1 - \frac{\sum_i (y_i - \hat{y}_i)^2}{\sum_i (y_i - \bar{y})^2}$$

where y_i are the observed values, \hat{y}_i are the predicted values from the regression model, and \bar{y} denotes the mean of y_i . Higher values of R^2 indicate a stronger adherence to a power-law scaling relationship.

Table 1: Empirical scaling exponents and goodness-of-fit metrics from log-log runtime regression.

Algorithm	D	p	R^2
Ball Tree	100	0.533	0.858
FAISS		0.560	0.852
pyBallMapper	200	1.157	0.977
Ball Tree		1.307	0.961
FAISS	500	1.159	0.968
pyBallMapper		1.976	1.000
Ball Tree	1000	1.609	0.979
FAISS		1.432	0.963
pyBallMapper	10000	2.038	1.000
Ball Tree		1.744	0.990
FAISS	100000	1.696	0.968
pyBallMapper		2.045	1.000

Table 1 reports the empirical scaling exponent p and corresponding R^2 values for each algorithm across different dimensions. For all methods, the scaling exponent increases steadily with D , reflecting the growing computational burden imposed by high-dimensional data and illustrating the effect of the curse of dimensionality. As dimension increases, py-BallMapper approaches near-quadratic scaling, indicating that its runtime grows rapidly in high-dimensional settings. In contrast, FAISS and Ball Tree maintain substantially lower scaling components across all tested dimensions, demonstrating better scalability for large high-dimensional datasets. The consistently high R^2 values confirm that runtime is well described by a power law model in this regime.

Authors' Contributions

Jay-Anne was responsible for drafting the manuscript, conducting benchmark experiments, and producing the data visualizations.

John Rick was responsible for drafting the manuscript, and programming the proposed algorithms.

Bibliography

- [1] R. Bellman, *Dynamic Programming*. Dover Publications, 1957.
- [2] P. Dłotko, “Ball mapper: a shape summary for topological data analysis.” [Online]. Available: <https://arxiv.org/abs/1901.07410>
- [3] K. Borsuk, “On the imbedding of systems of compacta in simplicial complexes,” *Fundamenta Mathematicae*, vol. 35, no. 1, pp. 217–234, 1948, [Online]. Available: <http://eudml.org/doc/213158>
- [4] T. F. Gonzalez, “Clustering to minimize the maximum intercluster distance,” *Theoretical Computer Science*, vol. 38, pp. 293–306, 1985, doi: [https://doi.org/10.1016/0304-3975\(85\)90224-5](https://doi.org/10.1016/0304-3975(85)90224-5).
- [5] S. M. Omohundro, “Five Balltree Construction Algorithms,” technical report TR-89–63, Dec. 1989.
- [6] F. Pedregosa *et al.*, “Scikit-learn: Machine Learning in Python,” *Journal of Machine Learning Research*, vol. 12, pp. 2825–2830, 2011.
- [7] M. Douze *et al.*, “The Faiss library.” [Online]. Available: <https://arxiv.org/abs/2401.08281>
- [8] B. Furht, Ed., “SIMD (Single Instruction Multiple Data Processing),” in *Encyclopedia of Multimedia*, Boston, MA: Springer US, 2008, pp. 817–819. doi: [10.1007/978-0-387-78414-4_220](https://doi.org/10.1007/978-0-387-78414-4_220).
- [9] R. van de Geijn and K. Goto, “BLAS (Basic Linear Algebra Subprograms),” in *Encyclopedia of Parallel Computing*, D. Padua, Ed., Boston, MA: Springer US, 2011, pp. 157–164. doi: [10.1007/978-0-387-09766-4_84](https://doi.org/10.1007/978-0-387-09766-4_84).